Macromolecules
ARTICLE

Macromolecules **2009**, *42*, 6181–6192 **6181**
DOI: 10.1021/ma802488a

Linear Viscoelastic Rheology of Moderately Entangled Telechelic Polybutadiene Temporary Networks

Florian J. Stadler,*,† Wim Pyckhout-Hintzen,‡ Jean-Marc Schumers,§ Charles-André Fustin,§ Jean-François Gohy,§ and Christian Bailly*,†

†*Unité de Physique et de Chimie des Hauts Polymères, Université catholique de Louvain, B-1348 Louvain-la-Neuve, Belgium,* ‡*Institute of Solid State Research, Research Center Jülich, D-52425 Jülich, Germany, and* §*Unité de Chimie des Matériaux Inorganiques et Organiques, Université catholique de Louvain, Place L. Pasteur 1, B-1348 Louvain-la-Neuve, Belgium*

Received November 6, 2008; Revised Manuscript Received July 13, 2009

ABSTRACT: We investigate the time-dependent linear viscoelastic behavior of amine and alkaline metal-neutralized carboxy−telechelic 1,4-polybutadiene, and compare it with the acid precursor as well as an ester end-modified version. The ionic groups form aggregates with a aggregate spacing period around 85 Å, containing about 90 chain-ends. Rheological tests highlight the existence of a strongly time-dependent terminal relaxation and an intermediate frequency relaxation, which can be assimilated to a glass transition of the ionic aggregates and their immediate environment. The terminal relaxation time after neutralization with alkali metal increases by up to 7 decades. Contrary to previously published results, this time is found to be a strongly increasing function of metal atomic mass for the equilibrated structures. The discrepancy can be rationalized by analyzing the annealing time dependence of the phenomena. Earlier studies did not report on truly equilibrated systems. While the main phase glass transition is hardly affected by neutralization, the temporary network formed by the ionic associations shows a very high and ion-dependent temperature sensitivity. Moreover, a failure of the time−temperature superposition principle is found at intermediate temperatures or frequencies, because the terminal and intermediate frequency relaxations do not follow the same temperature dependence.

Introduction

Apolar covalent polymer systems comprising polar supramolecular bonds have a rich variety of structure, dynamics, and widespread applications in bulk and solution. These polymers rely on relatively weak chemical interactions such as hydrogen or ionic bonds, to form temporary associations or networks, whose behavior is quite distinct from classical topological interactions (entanglements), observed in ordinary polymers. The supramolecular bonds have a characteristic lifetime, thus making the temporary network able to flow at times larger than this terminal time. Both entangled and unentangled supramolecular systems can be found in literature.

Much literature has been published in the field of *ionomers*, polymers with randomly distributed ionic groups along the chain. Because of the vastness of this topic, we restrict ourselves to a brief discussion of ionomers and telechelics melts.

Research on ionomers started in the 1960s. The introduction of ionic groups leads to a lengthening of the relaxation time scale, which is a consequence of the temporary network formation. Most research has been carried out on random copolymers of hydrophobic monomers with acid group containing monomers (e.g., sulfonic or carboxylic acid). If the ionic group content exceeds 5 mol %, a clear second glass transition is observed, which has been attributed to the existence of an ion-rich phase due to intramolecular phase separation. Depending on ion content and structure, ionic multiplets and clusters are found.[1−3]

It is generally agreed that clusters are formed at higher ion contents,[4] but the structure is heavily debated (core−shell vs large multiplets).[2] Although the origin of the second glass transition has to be attributed to the presence of ionic groups, the exact mechanism is still elusive as well as the physical origin of the SAXS-patterns observed. In terms of rheological properties, this second glass transition leads to two "rubbery plateaus", where the upper one actually reflects a composite behavior, as the ionic clusters phase is still glassy.

Telechelic polymers possess a much better defined structure by comparison with classical ionomers, as they contain the functional associating groups only at the chain ends. Not much rheological characterization has been performed so far, and, for the most part, in solution.[5,6] Research on telechelic systems started with a series of papers by the group of Jérôme,[7−10] who characterized the influence of different metal ions on carboxy-telechelic matrices by rheology (among other methods). The material behavior, including temperature dependence, was strongly dependent on the ionic bond strength and on metal valence. Broze et al.[8] further observed that intramolecular steric hindrance and high ionic groups concentration increase the terminal relaxation time for samples with less than two entanglements but no longer play a significant role at higher molar masses. The groups of Fetters, Graessley, and Hadjichristidis[6,11] identified one feature of telechelic networks, making them hard to characterize: a very long time dependence of the network structure, sometimes to be measured in terms of weeks. They also showed that telechelic polymers with monovalent metal carboxylate end-groups do not behave as star-like polymers as expected but instead as more hierarchal structures, which would correspond to H-polymers. This was attributed to the formation of clusters with several dozen chains attached to each other thus forming less mobile inner segments. A good overview of the

*Corresponding authors. (F.J.S) E-mail: florian.stadler@uclovain.be; floohneh@gmx.de.(C.B) E-mail: Christian.bailly@uclovain.be. Telephone: +32 10 47 3560.

Published on Web 07/24/2009

literature on ionic telechelic materials was published by Register and Prud'homme.[12]

The groups of Sillescu and Pakula[13,14] published an extensive discussion about the possible structures of telechelic systems. In general, an intramolecular phase separation has to occur, as the main chain is a nonpolar polymer, while the telechelic groups are polar. Thus, the general consensus is that the telechelic network is made up of domains of polar and of nonpolar groups (e.g., refs 15−17). These domains were characterized by SAXS (e.g., Hadjichristidis et al.[16]) and SANS (e.g., Karayianni et al.[18]), but one of the important still partially unanswered questions is to what degree the telechelic groups have inter- and intrachain interactions: i.e., how many of the chains form rings or bridges between different domains?[13,16] Shen et al.[19] reported a change from rod-like ion clusters to rather spherical ones in a bcc-lattice in zwitterionic PI when increasing the molar mass from 4650 to 14000 g/mol (1.5 → 3.0 times the molecular weight between entanglemens). By annealing another transition to a less ordered state was observed for the high molecular weight systems—a process which takes several days to complete, because of the pinning of the zwitterionic chain ends in ionic domains phase separated from the matrix.

The groups of Rubinstein and Leibler[20−22] have been very active in describing the rheological behavior of telechelic systems by models based on sticky reptation[20,23−25] and bridged micelles.[26] Recently, van Ruymbeke et al.[27] were able to successfully model the linear viscoelastic data of star polymers with 1 to 3 telechelic end groups using a statistical sticker approach, assuming a certain distribution of supra-molecules.[28]

Motivation and Aims. While (semi-) dilute solutions of telechelic polymers are relatively well characterized, the rheological behavior of concentrated solutions and bulk ionic telechelic polymers is still not very well understood. This is largely due to the scarcity of samples and the experimental difficulties usually associated with the extensive time dependence of the network structures.[6] Very few thorough rheological studies have been published. In particular, the time and temperature dependence deserve a more in-depth look. Elongational properties of telechelic networks have not been described at all to the best of our knowledge, while some are known for ionomers.[29]

The goal of this paper is to improve the understanding of telechelic networks structure and dynamic behavior by performing a thorough rheological characterization complemented by structural characterization on a dicarboxylic telechelic polybutadiene neutralized with different ions. The diacid precursor is moderately entangled (approximately 7 entanglements per chain, based on M_w), which should allow to explore the balance between topological and supramolecular interactions (at least for the weakest systems). The main focus will be on the ion, time, and temperature dependences of relaxation processes as well as the supramolecular structure.

Experimental Section

The commercially available material Hycar CTB 2000 x 162 ("acid precursor") from Emerald Materials was taken as the base for the investigations. According to the supplier, this material is made by radical polymerization. The composition of the acid precursor material is summarized in Table 1. The temporary networks were created by making a 10% solution of the acid precursor in a 90/10 mixture of toluene and ethanol as suggested by Davidson et al.[6] Also 1% of Irganox 1010 and 1% of Irgafos 168 (both from Ciba SC) were added to prevent degradation. The solutions were stirred for at least 6 h prior to neutralization.

The terminal COOH groups were neutralized stoichiometrically by alkali metal hydroxides in ethanolic solution, i.e., two mol of hydroxide was added per mol polymer, and stirred for 24 h. Lithium, sodium, potassium, and rubidium hydroxide were used in this study. After neutralization, the solvent was evaporated under ambient conditions for 2−3 weeks, next in vacuo at room temperature for 1 week and finally for 5 days in vacuo at 80 °C until the weight was constant.

Table 1. Material Composition[a]

material	*cis*-1,4-PBd (about 80%)
M_n	4.2 kg/mol
M_w	7.4 kg/mol
M_w/M_n	1.9
end groups	1.95 carboxy (−COOH) groups per chain

[a] M_w = weight average molar mass. M_n = number average molar mass. M_w/M_n = polydispersity index.

Additionally, the specific influence of carboxylic acid endgroups was assessed by comparing the rheological behavior of the acid precursor and ethyl ester versions of the same polymers. The esterification was performed as follows. At 0 °C and under argon, $(COCl)_2$ (3.3 mL, 39.05 mol, 20 equiv.) was added dropwise to a stirred solution of $PBd(COOH)_2$ (8.2 g, 1.95 mmol, 1 equiv) in dry CH_2Cl_2 (160 mL). Then, 20−22 drops of DMF were added. The mixture was stirred during 15 h at 20 °C. At 0 °C, dry EtOH (35.5 mL, 976 mmol, 500 equiv) and dry Et_3N (7.2 mL, 976 mmol, 500 equiv) were slowly added and the reaction medium was stirred during 48 h at 20 °C. The mixture was then washed with water. The organic layer was dried on Na_2SO_4, filtered, and concentrated in vacuo. The residue was precipitated in MeOH affording a light brown and highly viscous liquid. The polymer was dried one night in vacuo (7.5 g, 91%). ^{1}H NMR data were acquired on a Bruker Avance II 300 MHz. Chemical shifts are reported in ppm relative to the residual solvent peak ($CDCl_3$). ^{1}H NMR: δ 5.7−4.8(m, alkene H), 4.15 (q, ^3J = 7.1 Hz, −COO-CH_2CH_3), 2.6−0.7 (m, alkyl H).

SAXS studies were performed using a NANOSTAR camera (Bruker AXS) at the Institute for Solid State Research, FZ Jülich, Germany. The instrument was equipped with a rotating anode source, run at 40 kV and 40 mA and filtered to yield only Cu Kα with wavelength λ = 1.540 Å. The collimation path consisted of 3 pinholes. The primary beamstop at about 1.05 m from the sample position was 2 mm in diameter to allow the smallest scattering vector $q = 4\pi/\lambda \sin(\theta/2) \sim 0.006$ Å^{-1}, with θ being the scattering angle. Two-dimensional scattering patterns were collected on a Hi-Star Xenon-filled 1000 × 1000 wired grid area detector. Transmissions were obtained from absorbance measurements using a glassy carbon standard which was inserted in the optical path between sample and detector. The spot size of the beam on the sample was 500 μm. All data were corrected for detector sensitivity, background scattering, and dark current noise after a radially averaging process of the time-normalized data to yield a usable scattering vector range $0.006 < q < 0.20$ Å^{-1}. No absolute calibration was attempted for the analysis of the intensities due to the impossibility of measuring accurate thicknesses of the rubbery material, which was between 0.5 and 1 mm, approximately. In the small angle limit, excess intensity is noticed, typical for catalyst residues or voids since the sample chamber is evacuated. It is not further considered. Its intensity $I(q)$ follows $\sim Pq^{-\alpha}$ with α = 4. For the scope of the paper, no absolute cross sections are required and amplitudes of scattering as well as background are treated as fit parameters.

The rheological testing was performed on an ARES from TA Instruments. A 50, 25, or 8 mm parallel plate setup was used depending on the viscosity of the sample at a given temperature. The tests were carried out at temperatures between −90 and +100 °C using nitrogen cooling. The data were corrected for tool compliance effects according to the method described by Liu et al.[30] and by Sternstein[31] (which is only necessary for $|G^*| > 10^7$ Pa with an 8 mm geometry) and for density changes. Smaller plates would have decreased the accuracy dramatically and, furthermore, would have a very low sensitivity at low moduli.

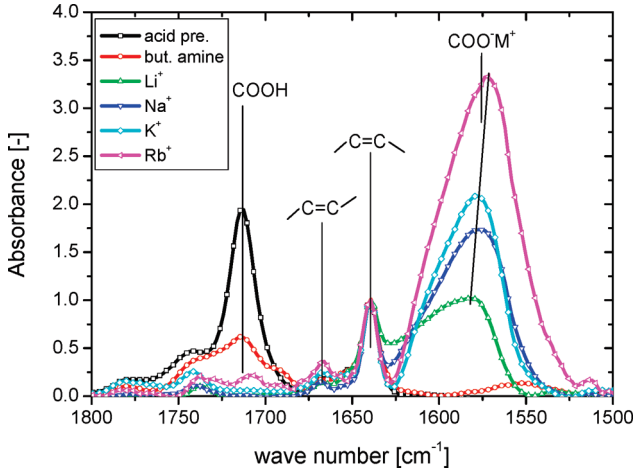

Figure 1. FT-IR-spectra of precursor and neutralized telechelic polybutadiene. Absorbance spectra were normalized to the *cis*-C=C peak (≈1640 cm^{-1}). The addition of ions leads to the disappearance of the COOH-band and to the appearance of the COO^-M^+ band.

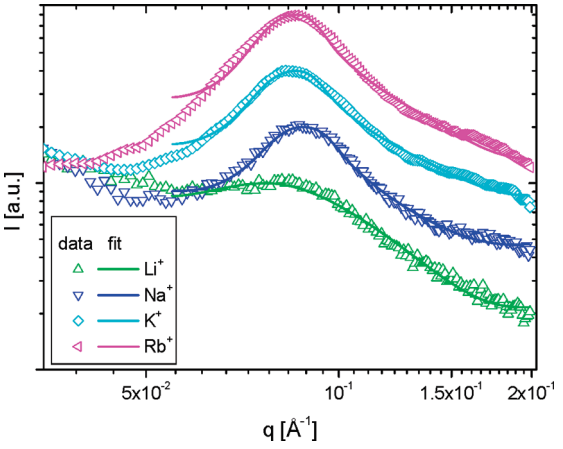

Figure 2. SAXS data in *q*-space of neutralized telechelic polybutadiene. The data are normalized to the height of the peak of the micro domain period and then staggered by a factor of 2 . The low *q* upturn is most likely caused by micro voids in the sample.

Additioonally, because of the long annealing, it is very difficult to remove the sample from the geometry and place it into a new one. The data were horizontally shifted to the glass transition temperature T_g (cf. Table 3).

For resetting the structure, a roughly ball-shaped sample was placed between two nonstick polyimide sheets and squeezed until it was fully flat. Then the spherical shape was restored manually and reprocessed again. The total treatment was repeated for about 5 min and should physically be similar to repeated 2-roll milling.

DSC-measurements were performed on a Mettler-Toledo DSC 821e at a heating rate of 10 K/min to determine the glass transition temperature.

The FT-IR-measurements were performed on a Nicolet Magna 720 IR in reflection mode through a microscope. The spectra were obtained by averaging 120 individual raw spectra with background subtraction.

Results

FT-IR. FT-IR measurements were performed to check whether the neutralization was complete and whether the neutralization procedure led to other chemical modifications than the desired ones. As can be seen from the comparison of the acid precursor and the neutralized samples (Figure 1), neutralization only leads to the complete disappearance of the COOH peak (at 1708 cm^{-1}) and to a new peak, associated with the ionic salt bond COO^-M^+ (M stands for a metal ion). The position of this new peak (around 1575 cm^{-1}) is located at slightly decreasing wavenumber with increasing ion atomic number. Otherwise, no significant spectrum change is found. However, the samples neutralized with the heavy ions potassium and rubidium show some traces of water (too low to quantify), which can be interpreted as the remainder of the hydration shell of these ions. Hence, water could not be fully removed during solvent evaporation for these samples, although they were extensively dried (see Experimental Section for details).

The COO^-M^+ peak becomes more pronounced (as compared to the neighboring *cis*-C=C peak, to which the data were normalized) with increasing atomic number of the ion. This is the consequence of the higher dipole moment of the COO^-M^+ bond with increasing metal atomic number.

For the butyl amine neutralized sample, the COOH peak is only reduced but is still present, indicating that neutralization is not complete despite a stoichiometric amount of amine used. This material also does not show the usual salt peak but a smaller one around 1550 cm^{-1}, which is associated to the weaker the coupling of the COOH and butyl amine groups, in agreement with earlier findings that such small organic ions lead to quite weak ionomeric interactions.[1] In addition, a possible explanation could also be the partial evaporation of butyl amine during evaporation of the solvent.

Finally, FT-IR also shows the presence of small amounts of anhydrides in the sample (around 1780 cm^{-1}).

SAXS. Figure 2 shows typical scattering patterns as a function of the ion. There is a clear diffraction peak visible, the position of which shifts, depending on the polymer and the type of ion and of a shoulder located at $1.42q_{peak}$. This observation is similar to that made by Shen et al.[19] for annealed telechelic zwitterion polyisoprene with a molecular weight of 14000 g/mol, which corresponds to approximately to 4 entanglements per chain and thus to a molar mass of 6000 g/mol for PBd. Shen et al. interpret their observations as the evidence of a BCC-lattice.

Similarly, we favor the assumption of a lattice-like BCC arrangement of ionic clusters in the amorphous matrix, as opposed to the hard-sphere interaction model, used earlier for the description of more random-distributed ionomers.[32] The peak can, therefore, be related to a Bragg distance, reflecting the average interdistance between clusters. A rough estimate of this interdistance of aggregated ions is $a = 2\pi/q_{peak}$, which is approximately 50−100 Å in the present samples.[32,33]

We also performed measurements on mechanically pretreated samples (such as described in the Experimental Section). However, we did not find a dramatic change in the scattering as one would expect from such an intensive mechanical treatment. The scattering peak gets slightly broader but the position remains identical. This is a very strong indicator that the cluster structure is distorted but not destroyed by the mechanical treatment.

The intensity measured by SAXS contains both the form factor of the small ionic aggregates and the structure factor of the ensemble of the domains. The model, which we adopted, is based on spherical ion aggregates, which are dispersed in a hydrocarbon matrix and arranged in a BCC lattice.[16,19] The ionic aggregates, which are more-or-less core−shell type particles and chemically inhomogeneous as well as polydisperse, are averaged over their volume. For their supramolecular arrangement, we adopt the paracrystalline distorted

Table 2. Fits with Paracrystalline Model of Hosemann[34] in the Representation of Matsuoka et al.[35,36]/bcc[a]

ion	R_m [Å]	a [Å]	$\Delta a/a$
Li^+	23.8 ± 0.06	83.3 ± 1.1	0.340 ± 0.004
Na^+	24.0 ± 0.07	92.1 ± 0.18	0.187 ± 0.001
K^+	22.0 ± 0.2	96.6 ± 0.2	0.183 ± 0.001
Rb^+	21.9 ± 0.15	96.9 ± 0.2	0.170 ± 0.001

[a] The cube dimension parameter "a" and its relative fluctuation $\Delta a/a$ are fitted as well as the Gaussian-distributed mean-size radius of the aggregates. Notice that the fluctuations Δa are roughly 15−20 Å and correlate well with the form factor parameter, R_m, i.e., both agree whether determined from either $P(q)$ or $Z(q)$. The first number in each cell is the fitted value; the second one refers to the uncertainty of this value. The fits of the aggregate dimensions in Table 2 are not to be over-interpreted and serve merely to illustrate how the lattice could look like.

lattice model[34−36] in analogy with classical colloidal systems and microphase separated blockcopolymers. More recent refined structures from, e.g., PRISM theory, do not seem to apply here and are not straightforward to use. Details of the calculations[34−36] are not repeated here. In brief, the orientationally averaged structure factor

$$I(q) = \langle C\langle P(q)\rangle_R Z(q)\rangle_{orient} \quad (1)$$

is calculated. C is a constant, which depends on concentration, scattering centers, and contrast as well as flux parameters and is optimized as a scaling prefactor.

A spherical form factor $P(q)$ for the ionic clusters with a Gaussian size distribution function:

$$w(R) = \exp(-(R-R_{mean})^2/2\sigma^2)/(2\pi\sigma)^{1/2} \quad (2)$$

and

$$\langle P(q)\rangle_R = \int_0^\infty w(R)(4\pi/3)R^3(3(\sin(qR) - qR\cos(qR))/(qR)^3)^2\,dR/\int_0^\infty w(R)\,dR \quad (3)$$

is included. The integrals are evaluated numerically. In the low q, the range form factor reduces to the simple Guinier function

$$I(q) = I_0\exp(-(qR)^2/5) \quad (4)$$

The orientationally averaged lattice-dependent structure factor Z(q), is, however, a sensitive function of the lattice parameter "a", i.e. the distance between the clusters, and its distortion or fluctuation "Δa" about the assumed ideal lattice. For relative large distortions $\Delta a/a \sim 0.15$ (see Table 2), in the accessed q-range, only two peaks are expected with estimated relative heights of 3:1. In figure 2 the second peak is indicated by the shoulder around 0.13 Å, i.e., $1.42q_{peak}$. The intensity ratio is reduced due to the underlying form factor of the aggregate. If the latter is approximated by the Guinier function (for illustrative reasons only), the second order peak intensity is increased by about 25%. For the calculation, a mean radius of 20 Å, coherent with Table 2 values, is used.

The microdomain period ("a") is approximately 90 Å (Table 2) and allows for an estimate of the number of ions and chain ends per cluster. As the number average molar mass M_n is approximately 4.2 kg/mol, there is about one acid endgroup per 120 carbons. This yields 2.6×10^{26} ionic groups per m^3, assuming stoichiometric neutralization. The microdomain period value, under the assumption of a bcc-lattice, means that 1.37×10^{24} unit cells are present per m^3. Hence, 188 salt groups are statistically present per unit cell. The bcc-unit cell contains two clusters, thus, approximately 90 salt groups form one cluster. Under the assumption of cubic clusters, this number would be equivalent to a cube with a little less than 5 salt groups along each axis. However, this ideal arrangement is certainly unrealistic, as the clusters are distorted spheres and presumably contain some portions of apolar backbone (which we cannot check because we cannot rely on the absolute SAXS intensities), but the simplified approximation leads to the conclusion that the number of 90 salt groups per cluster is realistic.

Table 3. Glass Transition Temperatures Determined by DSC and Rheology

	T_g^{DSC}	T_g^{rheo}
acid precursor	−77.0	−77.5
esterified material	n.d.	−79.8
BuAmine	n.d.	−78.1
Li^+	−78.6	−78.9
Na^+	−79.4	−78.2
K^+	−78.6	−78.5
Rb^+	−79.0	−79.8

The distance between the clusters (middle to middle ≈90 Å) is distinctly smaller than the length of the stretched chains, which would be more than 200 Å (depending on the ratio of 1,4 and 1,2 insertion). This also makes sense, as the stretched conformation of a chain is very unlikely for entropic reasons.

Glass Transition. Two different methods were applied to measure the glass transition temperature T_g. The standard method was a DSC-measurement, where the midpoint of the glass transition is taken as T_g. As a confirmation, T_g was also determined from the peak of $G''(a_T \times \omega)$ after compliance correction. The glass transition temperature from rheology T_g^{rheo} is defined as the temperature where the glassy peak is located at an angular frequency of 1 s^{-1}. From the reproducibility of both methods we conclude that the accuracy on T_g is around ± 1 °C and that the two methods agree remarkably well with each other.

As can be seen from Table 3, neutralization decreases T_g by maximum 1 K (probably not significant). Esterification decreases T_g by a marginally significant 2 K.

No secondary glass transition, as usually found in ionomers with high ionic content (3 mol % or higher,[1,2]) was observed by DSC (and also not by mDSC), probably owing to the low ionic content (approximately 0.7 mol %).

Rheology. *Influence of the Carboxyl End-Groups.* Figure 3 shows the linear viscoelastic data (master curves at T_g) of the acid precursor $PBd(COOH)_2$ and the esterified version $PBd(COOEt)_2$. It is obvious that esterification leads to distinct rheological properties in the rubbery and terminal regions, while the glass transition is essentially unchanged. Esterification leads to a decrease of the terminal time by a little more than one decade, which means that $PBd(COOH)_2$ already shows the onset of supramolecular bonding (H-bond dimerization of the acid groups), which is destroyed by esterification.

A comparison with two almost monodisperse polybutadienes (PBd 6k and PBD 14k) with molar masses of 6 and 14 kg/mol respectively is also shown in Figure 3.[37,38] The esterified sample has a slightly longer reptation time than PBd 6k (red lines),[38] which is logical considering the weight average molar mass of the esterified sample (M_w = 7.4 kg/mol). Also the data for the monodisperse sample shows sharper transitions, which is consistent with the

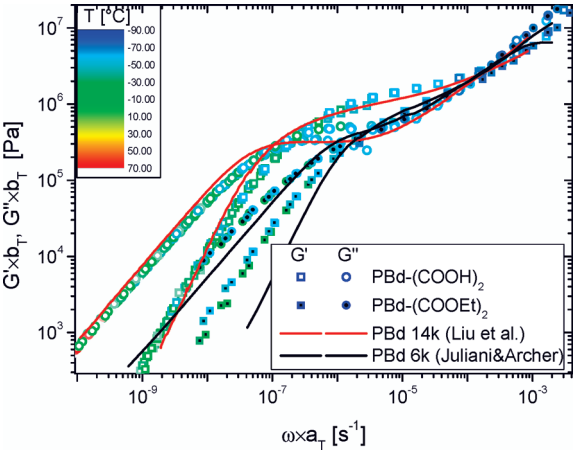

Figure 3. Comparison between the linear viscoelastic data of the acid precursor PBd(COOH)$_2$, esterified PBd(COOEt)$_2$, and low molar mass monodisperse PBd.[37,38] Temperature range: −90 to −10 °C (esterified sample); −90 to +10 °C (acid precursor). Reference temperature is T_g.

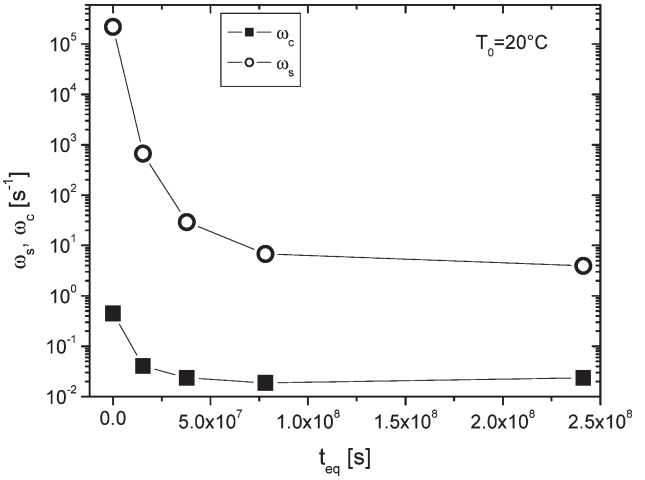

Figure 4. Equivalent time-dependence of the crossover-frequency ω_c and of the secondary relaxation frequency ω_s for the potassium neutralized sample (T_0 = 20 °C).

broader molar mass distribution of the PBd(COOH)$_2$ sample ($M_w/M_n \approx 1.9$).

The acid precursor material shows a very similar behavior to PBd 14k (dashed lines)[37] except at the lowest end of the terminal region (see below). In a very much simplified picture this would mean that PBd(COOH)$_2$ acts as a material with double the acid precursor's molar mass. However, there is no reason to believe that this is a realistic image. The real situation is rather a dynamic equilibrium of dimerized and non dimerized COOH groups with a characteristic lifetime around the reptation time of PBd 14k (about $\tau_d = 2 \times 10^6$ s—relative to T_g).[37]

The acid precursor sample has another interesting feature. Its plateau modulus G_N^0 is somewhat higher than that of the monodisperse counterpart and also higher than of the esterified sample, which is another indicator for the presence of a weak network in the acid sample.

Time-Dependence of the Rheological Properties. *Equivalent Equilibration Time.* The neutralized samples exhibit a clear "equilibration" time dependence of the rheological properties. To assess this properly, we used a systematic preparation procedure, in which the samples were intensively hammered for 5 min before loading in the rheometer, in order to "reset" the supramolecular structure as effectively as possible. As the time to reach equilibrium was very long for some systems, we systematically varied the temperature during measurement programs in order to speed up the process. Hence, we used a global indicator of the equilibration time, which we call equivalent time, t_{eq}, defined as the sum of corrected measurement times obtained by dividing the actual time of the experiment (t_i) by the shift factor corresponding to the experiment temperature and time, i.e.:

$$t_{eq} = \sum \frac{t_i}{a_{T_i}(T)} \tag{5}$$

A discussion on the shift factors is presented later. This equivalent time was next used to find out the approximate equilibration time dependence of the different relaxation processes. The results are presented in Figure 4 for the K neutralized sample but the findings are similar for other alkaline metal cations, although the time scale varies. The heavier the ion the longer it takes to reach equilibrium. For the butyl amine neutralized sample, the acid precursor, and the esterified sample no time dependencies were observed. This is the consequence of their low viscosity at room temperature, which makes the annealing time too fast to be observable in a rheometer.

Figure 4 shows the time dependence of the crossover frequency ω_c, corresponding to the terminal relaxation, and of a secondary relaxation frequency ω_s, corresponding to the small loss modulus shoulder located around 10^{-6} s^{-1} at short equilibration times on the mastercurve (Figure 5a). Its origin will be discussed in detail later on. Both processes become distinctly slower with increasing time, but the secondary relaxation shows a much stronger dependence of the equivalent equilibration time than the terminal relaxation.

In the initial "reset" state as well as the equilibrated state, three main relaxations can be observed from the dynamic modulus curves and the van Gurp−Palmen plots ($\delta(|G^*|)$). Figure 5 and 6 show the results for the K, Rb, and acid precursor, respectively (the same observations were made for all ionic samples). The glass transition lies at the highest frequencies (or moduli when looking at $\delta(|G^*|)$). At intermediate frequencies, a secondary relaxation is observed as a small shoulder on the loss modulus curve. This relaxation is barely visible in the $\delta(|G^*|)$ plot because of the small modulus change. The relaxation separates "high" and "low" regions of the plateau modulus. This is best seen on the van Gurp−Palmen plots (minimum and shoulder in the plateau region) and is more evident for reset than for equilibrated samples (Figure 5b and 6b). The plateau moduli in Figure 5 and 6 were determined from the minima in the van Gurp−Palmen plots. Finally, a terminal relaxation regime is observed for all samples. The two latter relaxations are discussed in more detail below.

Intermediate Relaxation and Plateau Modulus. Considering that the intermediate shoulder is not present in "normal" polymers, this relaxation is presumably linked to the presence of clusters. As indicated earlier, its location depends more on annealing time than that of the terminal relaxation. This suggests that annealing perfects the "short range" cluster structure more significantly than the long-range cluster arrangement. Conversely, it also means that the mechanical treatment destroys the short-range structure much more than the long-range arrangement. This is in agreement with the finding that the SAXS pattern is not distinctly influenced by the mechanical treatment (the peak gets slightly broader, but does not change its position).

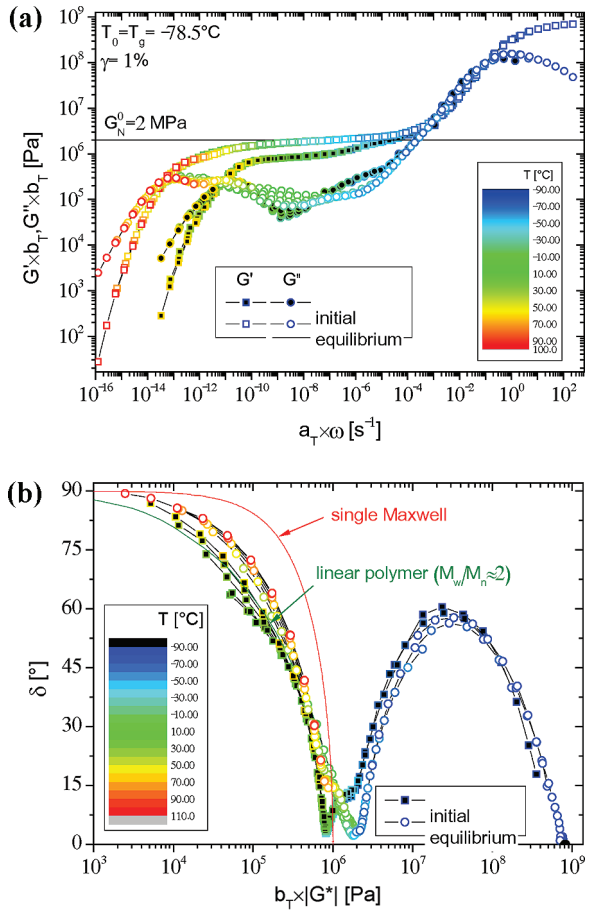

Figure 5. Rheological data of the potassium hydroxide neutralized sample. Black-filled symbols refer to initial state (about t_{eq} = 300 s) and the white filled samples refer to the equilibrium state after about t_{eq} = 2.4 × 10^8 s). Temperature range: −90 to +50 °C (initial), −90 to +100 °C (equilibrium). Key: (a) complex moduli; (b) $\delta(|G^*|)$ plot (the linear reference for PE was established elsewhere).[49,50] Reference temperature is T_g.

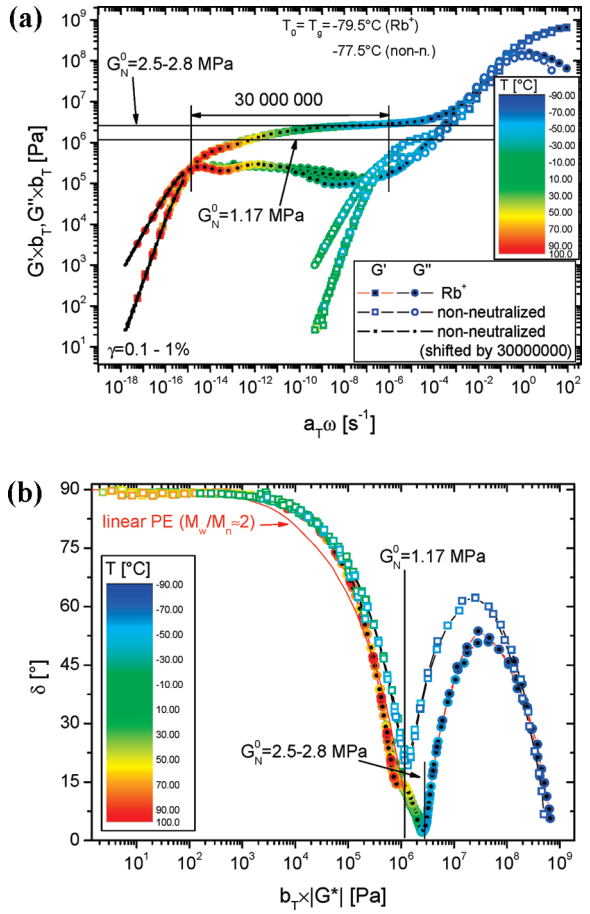

Figure 6. Apparent dynamic modulus master curves of the acid precursor and of the rubidium neutralized samples. Black-filled symbols refer to the rubidium neutralized sample and the white filled samples refer to the acid precursor, the small black symbols are the data of the acid precursor shifted by a factor of 3 × 10^7. Temperature range: −90 to +100 °C (Rb^+), −90 to +10 °C (acid precursor). Key: (a) complex moduli ($T_0 = T_g$); (b) $\delta(|G^*|)$ plot.[49,50,52,53] Reference temperature is T_g.

Unlike normal PBd, the neutralized samples show a clear thermorheological complexity around the minimum of $G''(\omega)$, which is the generally accepted location of the rubbery plateau. This appears to be a typical feature of telechelic networks.[39−46] As the plateau is clearly influenced by the existence of ionic clusters, a logical explanation lies in a time and temperature dependence of the cluster structure. This will be clarified below by a discussion on shift factors.

The high end of the plateau modulus of the equilibrated samples is distinctly higher than the initial "reset" samples and also higher than reference data for normal PBd.[47] This is a good indication that the dynamics are no longer dominated by the chains themselves but that the telechelic interactions between chain ends contribute significantly to the network and lead to a composite behavior.

Terminal Relaxation. From examination of the van Gurp−Palmen plots in Figure 5b and 6b, it is clear that the terminal relaxation does not follow a single Maxwell-mode. Instead the terminal relaxation pattern is similar in shape to the acid precursor and the esterified sample. Hence, the terminal relaxation is most likely the combination of two processes. The first one is the break-up of the chain-cluster interaction followed by the normal relaxation of the detached chain. The chemical nature of the first process leads to narrow relaxation time distribution for the first part of the relaxation and, thus, leads to a slight narrowing of the total relaxation time distribution. These results are in general agreement with observations for other telechelic polymers, indicating that the material behavior is not governed by a simple (chemical) relaxation mechanism but by a more complicated pattern.[48] Figure 5b also shows that the terminal regime of the reset samples is thermorheologically complex, which can be explained by a structure evolution during the measurement itself. In particular, at higher temperature, the structure ordering processes become fast and thus relevant on the time scale of the experiment. The equilibrium states do not show this thermorheological complexity in the terminal regime.

The minor effect of the mechanical treatment to the cluster interdistance as observed by SAXS, clearly shows that this quantity has no relevance to the terminal regime.

Influence of the Counterion. The previous section was mainly concerned with the time dependence of the temporary network. From this point, all the samples are in equilibrium state. Figure 6 shows the effect of neutralization with Rb^+ on the complex moduli $G'(\omega)$ and $G''(\omega)$. The characteristic relaxation time (the inverse crossover frequency ω_c) is increased by a factor of approximately 3 × 10^7 (master curve at T_g). Interestingly, when shifting the terminal regime data of the acid precursor by this factor, we observe that the data superimpose almost perfectly, indicating that the terminal relaxation pattern is only slowed down but not otherwise affected by neutralization. The $\delta(|G^*|)$ plot shows this again, as both samples are

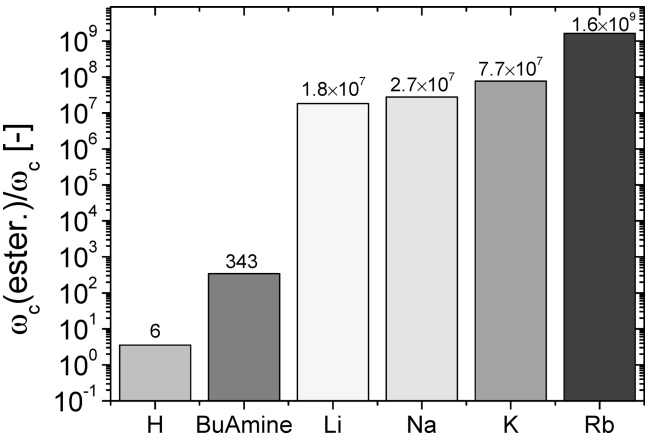

Figure 7. Influence of the counterion on the characteristic relaxation time (calculated for T_0 = 20 °C).

basically undistinguishable for $|G^*| < 10^6$ Pa, i.e., below the plateau modulus of PBd. The increase of the terminal relaxation time is in good agreement with previous findings.[12,51]

The shape of the data in the terminal regime is typical for a linear polymer.[52,53] However, as mentioned before, it is a little narrower in the transition from rubbery to terminal regime than PE with M_w/M_n = 2 (Figures 5 and 6). This indicates a small remaining influence of a first order process.

The plateau modulus determined for the acid precursor is 1.17 MPa, which is only slightly above typical values for ordinary PBd.[47] This indicates that the COOH groups alone do not have a large impact on the entanglement network, i.e., do not significantly increase the concentration of (temporary) cross-linking points.

For the Rb^+-neutralized sample, the main ("upper") plateau modulus is between 2.5 and 2.8 MPa,[54] which is much higher than the value found for normal PBd[47] and corresponds to an "apparent entanglement molar mass M_e'' of 700−800 g/mol, about one-third of the value of PBd. This indicates that the entanglement network is enhanced by the ionic clusters.

Another interesting finding is that the phase angle at the minimum of the $\delta(|G^*|)$ plot, corresponding to the rubbery plateau, shows a lower phase angle for the neutralized sample ($\delta \approx 2-5°$) than for the acid precursor ($\delta \approx 15°$). Trinkle and Friedrich[55] established that this minimum is directly correlated with the molar mass of an ordinary polymer. In our case, the molar mass is constant, but the strong ionic associations between the chains of the neutralized sample lead to a huge extension of the rubbery plateau region, explaining this lower minimum phase angle.

The influence of the neutralizing ion is clearly visible when looking at the shift of the characteristic crossover relaxation time ω_c^{-1} vs the crossover of the esterified sample, which has no supramolecular interactions (Figure 7). For the butyl amine-neutralized sample, a very weak effect is found, while for the other ions much stronger interactions are obvious. The characteristic relaxation time ω_c^{-1} of the alkali metal ion neutralized samples increases with atomic number from 1.8×10^7 for Li to 1.6×10^9 for Rb. This observation will be analyzed in more detail further on, leading to a better understanding of the processes occurring.

While the weak effect of organic amines is in good agreement with previous findings,[12] the alkali metal ion effect runs opposite to previous results.[7,12] However, the materials are very much time dependent, especially with respect to the perfectioning of the cluster phase structure, and there is an

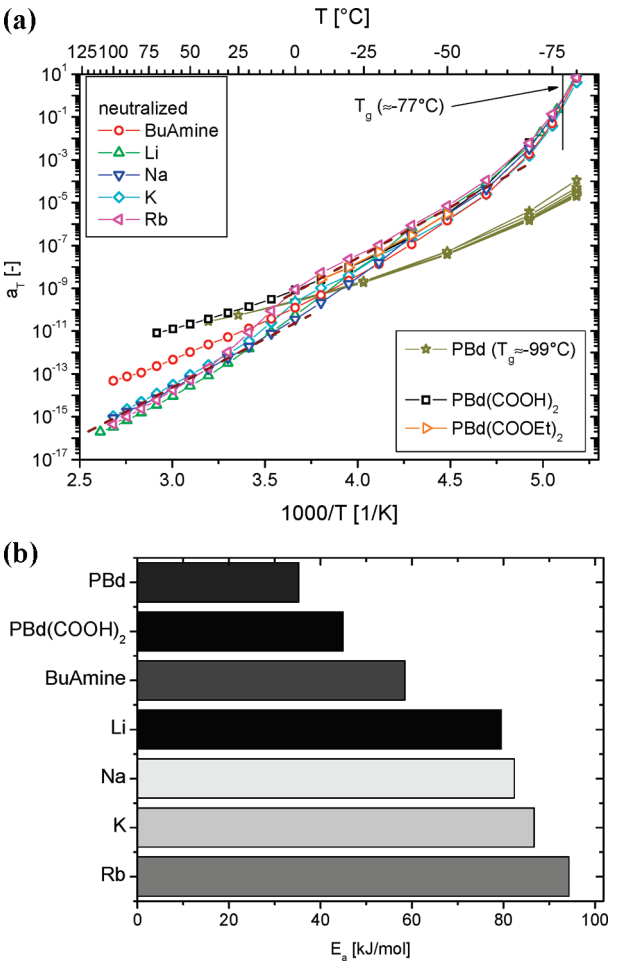

Figure 8. Shift factors of normal PBd, the acid precursor, and neutralized samples: (a) Arrhenius plots (normalized to T_g); (b) activation energies above room temperature.

atomic number dependence of this quantity as well. While the Li^+-neutralized sample was found to be in equilibrium after only a relatively short annealing time (about $t_{eq} = 3 \times 10^7$ s), the required time for reaching equilibrium of the heavy ion samples K^+ and Rb^+ was higher by a factor of more than a factor of 10. Hence, the ranking of terminal times vs ion atomic number seems to "flip around" between "reset" and equilibrated states. This effect was apparently not discovered before, as the required time is "longer than most researchers' patience"—as Register and Prud'homme[12] put it. The increase of the terminal relaxation time is also qualitatively related to the time necessary to reach the equilibrium state as discussed before (cf. Figure 4).

Temperature Dependence. The shift factors for the acid precursor, the esterified and the neutralized systems are presented in Figure 8a as an Arrhenius plot. Reference temperature is T_g. Several observations can be made.

First, the shift factors are strongly influenced by chain-ends and neutralization. While the shift factors of ordinary PBd and the esterified sample are very similar, the acid-terminated and neutralized systems show a much higher temperature dependence.

Second, it is useful to distinguish three broad temperature zones for the analysis of the shift factors: close to the glass transition (lower than −70 °C), in the approximate rubbery plateau region (above −70 °C but below room temperature) and in the terminal flow region (above room temperature.)

The slope around the glass transition corresponds to an activation energy of approximately 280−300 kJ/mol, a typical value for a glass transition. It does not depend on the counterion, nor on the annealing time.[56] The small observed differences around −40 °C between samples are due to minute differences in T_g. This behavior is consistent with the idea that the glass transition corresponds to the freezing of the chain segment movements and is thus not influenced by temporary links between chains.

In the rubbery plateau region, the shift factors are very dependent on the ion, but the slopes are similar. At −40 °C, for example, the Li^+-neutralized sample and the acid precursor sample differ by a factor of 60, when using $T = 25$ °C as reference temperature.

Using T_g as reference temperature collapses the shift factors of all samples below −50 °C (except for the literature data of the PBds, because these have a different T_g around −99 °C). Above −50 °C, the neutralized samples start deviating from the acid precursor. The heavier the ion the higher the temperature, at which a deviation is found. The deviation of the alkali metal ion neutralized samples increases the shift factors by about 1.5 decades (see dashed lines in Figure 8a), i.e. a process occurs which leads to an additional factor ≈30 in the temperature dependence. The BuAmine-neutralized sample is between the acid precursor and the alkali metal ion neutralized samples.

Above room temperature, the shift factors follow an Arrhenius type temperature dependence, which is strongly influenced by the nature of the ion. The corresponding activation energies E_a are given in Figure 8b. The acid precursor already has as significantly higher activation energy than normal or esterified PBd (from 38 kJ/mol to 45 kJ/mol).

The weakest counterion—butyl amine—causes further increase. The alkali metals have a much stronger influence, which increases with atomic number to up to 92 kJ/mol for the Rb^+-neutralized sample. As already mentioned before, the observed counterion dependence is inverted in comparison to previous findings,[7,12] but this can be explained by the same arguments on equilibration time as mentioned before.

Another way of looking at the temperature dependence is to check for the validity of universal scaling laws for the time−temperature superposition (TTS). Recently, Liu et al.[57] proposed a new method for the normalization of shift factors by using a T_g-rescaled temperature axis. Liu et al.[57] show the validity of this approach for a range of amorphous polymers, as they find an excellent linear correlation between $\log a_T$ and $T_g/(T - 0.77 \times T_g)$ with a universal slope of 3 over a wide temperature span (dashed line in Figure 9). A (non arbitrary) vertical shift factor A' accounts for T_g differences and allows to superimpose data for different polymers. This correlation is applied to the shift factors of the materials under discussion here. For the reference PBd data, T_g is taken to be −99.5 °C; for all other samples, we use the average T_g measured by rheology and DSC.

Figure 9 shows that the correlation is valid with good accuracy for the PBd reference and the $PBd(COOEt)_2$ over the entire experimental temperature range, while the validity of this correlation is restricted for the samples with ionic groups only up to a temperature of approximately −35 °C, indicated by the vertical line. The scatter around T_g is the consequence of the extremely high temperature sensitivity coupled with the slight uncertainty on temperature in this region (±0.2 °C). For temperatures above ≈−35 °C (depending on the ion used), the correlation clearly and systematically fails toward lower shift factors

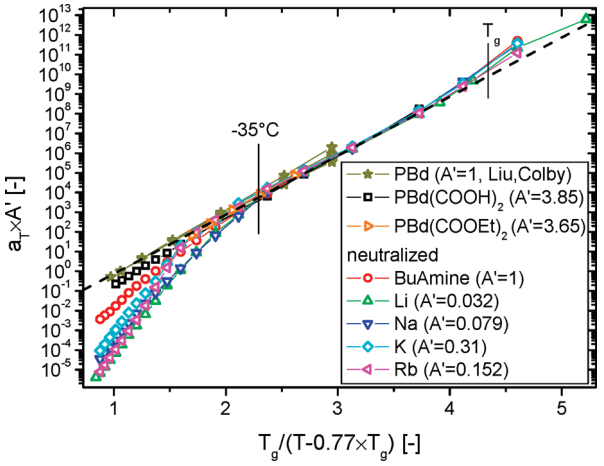

Figure 9. Universal normalized plots of the shift factors for the acid precursor and the neutralized samples in comparison to a standard polybutadiene.

i.e. a higher temperature dependence. Interestingly, the failure of universality corresponds to the onset temperature of thermorheological complexity (Figure 6a).

Such a dramatic failure has not been reported for ordinary covalent polymers and is obviously the consequence of additional relaxation processes, which are not occurring in "ordinary" polymers. We further observe that the precise location of the onset is ion-dependent and scales with the lengthening of the terminal relaxation time. In all cases the onset of the deviation from the "normal PBd" corresponds to the end of the "upper rubbery plateau" (between 1.8 and 2.8 MPa depending on the ion used). In other words, as soon as the supramolecular clusters become too weak to be counted rheologically as "cross-linkers" the temperature dependence starts becoming irregular.

In this irregular regime the slope is also material specific, reflecting the different activation energies in the terminal regime (cf. Figure 8b).

This irregular temperature dependence given in the universal plot (Figure 9) is also the reason why a WLF plot would not lead to additional insight, as any pure WLF-temperature dependence has to lie on the dashed line in Figure 9.

The systematic deviations of the shift factors in the universal plot (Figure 9) toward higher slopes above a certain threshold temperature raise the question, whether the high temperature processes perhaps follow a universal behavior related to another (higher) glass transition temperature, as T_g determines the slope in the universal normalized plot. Hence, T_g was set as a freely adjustable parameter to optimize the fit of the high temperature shift factors to the universal curve (with a slope of 3). The results are shown in Figure 10. As a consequence of the new glass transition choice, the shift factors at low temperatures no longer adhere to the universal relation, but show a distinctly smaller slope. All data deviating from the slope of 3 in Figure 9 can be moved onto the reference by this adjustment. The parameters (adjusted T_g' and A') are given in the legend of Figure 10. The values for the fitted T_g' increase from −65 °C for the acid precursor material to −5 °C for the Rb^+-neutralized one. These temperatures correspond to the temperature, at which the "upper" rubbery plateau ends (visible for the acid precursor as well as all the neutralized samples). For the acid precursor material, this corresponds to $a_T \times \omega \approx 10^{-5}$ s^{-1} and $a_T \times \omega \approx 10^{-10}$ s^{-1} for the Rb^+-neutralized material (for $T_0 = T_g$). It also corresponds to the position of

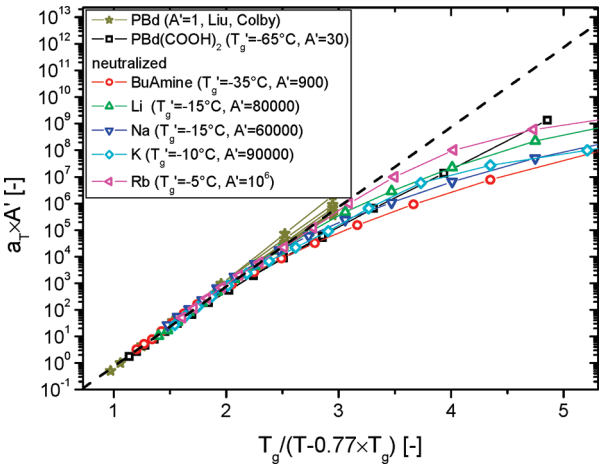

Figure 10. Universal normalized plots of the shift factors with fitted glass transition temperatures for the acid precursor and the neutralized samples in comparison to a standard polybutadiene.

the secondary relaxation process ω_s already discussed by reference to Figure 4.

These correlations confirm that T_g' is not just a freely adjustable parameter, but that it actually corresponds to a physical transition, the glass transition of the ionic clusters.

The "upper" plateau modulus is then the consequence of two processes directly related to the presence of glassy ionic clusters. First, the glassy clusters act as filler and thus increase the modulus. The low volume fraction makes this effect quite weak, however. Second, and more importantly, the glassy clusters arrest the mobility of the chains attached to them. Hence, the clusters can be considered as supercross-linkers or as hairy micelles with a hard, vitrified core below T_g'. Above T_g', the structure becomes soft and thus chains can move in and out of the cluster, which lessens their effect on the plateau modulus, thus leading to the "lower" plateau modulus and highlighting the thermorheological complexity.

Besides the influence of the neutralizing ion, also an equilibrium time dependence is observed for the shift factors. The data for the potassium neutralized sample in both initial and equilibrium state are given in Figure 11 as an Arrhenius plot. Comparison with the acid precursor shows that the K^+-neutralized sample initially has a temperature dependence relatively close to but slightly stronger than the acid precursor, while annealing to equilibrium leads to a much stronger temperature dependence for both the terminal and rubbery regions (Figure 11). The shift factors were determined from $G'(\omega)$ and $G''(\omega)$ with the greatest possible precision − ignoring the thermorheological complexity. Strictly speaking, this is not totally correct, but it is still possible to find a master curve with sufficient accuracy in terms of $G'(\omega)$, while the thermorheological complexity mostly resides with $G''(\omega)$, in agreement with the qualitative finding that the smaller part of $G^*(\omega)$—either $G'(\omega)$ or $G''(\omega)$—is more relevant for finding the structural features of a material.[58]

The activation energy in the terminal regime is annealing time dependent. In initial state it is around 72 kJ/mol and increases to its equilibrium value (≈90 kJ/mol) after an equivalent equilibration time (at 20 °C) $t_{eq} = 4 \times 10^7$ s.

The universal plot (normalized to the main T_g) shows that the shift factors at high temperatures do not follow the reference with a slope of 3 any more (see insert in Figure 11b).

Plotting the shift factors with the help of the "universal" plot referenced to cluster glass transition (Figure 11b) shows

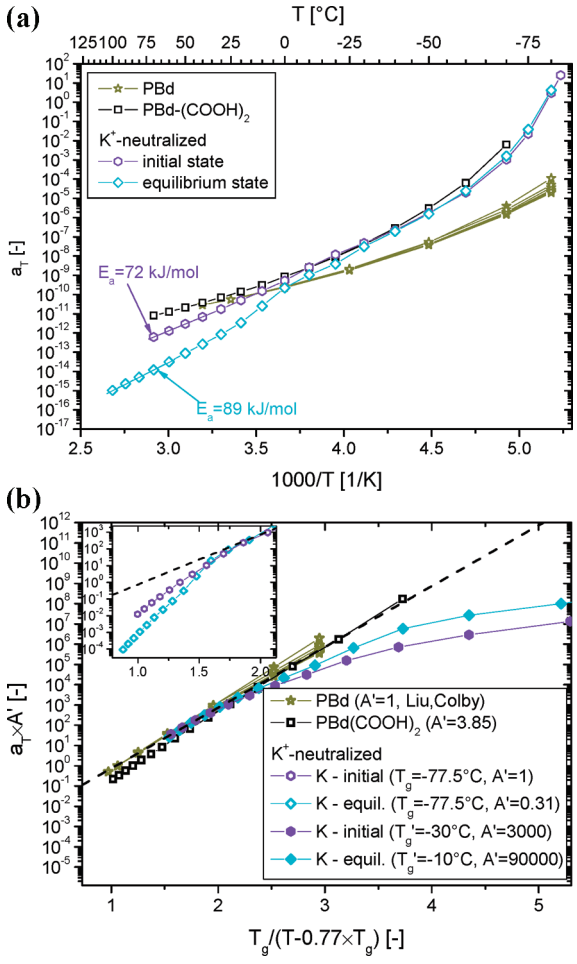

Figure 11. Time dependence of the shift factors with annealing time for the K^+-neutralized sample in comparison to the acid precursor and a standard polybutadiene: (a) Arrhenius plots; (b) universal normalized plot (for secondary T_g), insert: universal normalized plot for main T_g.

that the T_g' varies as a function of equivalent time, which is also reflected in Figure 5a as the distinctly different length of the "upper" plateau modulus. This time dependence reflects an aging process,[59] dominated by the perfectioning of the clusters.

This perfectioning - induced time dependence of T_g'—also clarifies the origin of the different position of T_g' for different ions in the equilibrated situation. More perfectly built clusters are reflected in a higher T_g' and a longer "upper" rubbery plateau. A highly ordered cluster structure such as for the Rb^+-neutralized material will consequently have a very high terminal relaxation time while the opposite is true for the acid precursor. Because a highly ordered cluster traps more chain ends than a disordered one, also the level of the "upper" plateau modulus is higher.

Connection between Terminal Relaxation Time and Molecular Structure. Figure 7 shows that the terminal relaxation time increases with increasing atomic number of the counterion. An explanation for this finding can only be obtained, however, from an insight into the molecular structure. The discussion around Figures 10 and 11 has already established that the neutralized samples show a second glass transition associated with the clusters, which is strongly related to the terminal relaxation time. To perform this comparison quantitatively, we need reference points which are not influenced by the ionic bonds. Hence, we define, on one hand, a shift factor between the cluster T_g' and the main T_g, as the latter is

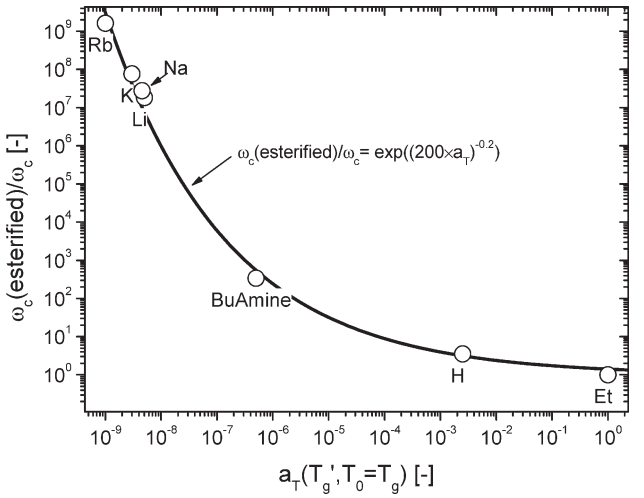

Figure 12. Crossover frequency ω_c as a function of the shift factor between T_g and T_g' for the neutralized samples and acid precursor relative to the esterified sample ($T_0 = T_g$). Line added to guide the eye.

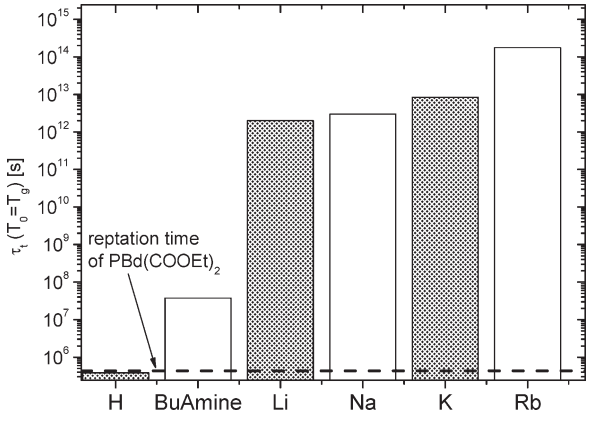

Figure 13. Characteristic life times of the telechelic association for the neutralized samples and the acid precursor.

hardly influenced by the ion, and, on the other hand, the ratio of terminal crossover frequencies for the ionic and esterified samples as the latter behaves like "normal" PBd. Figure 12 shows the relationship between these two quantities, which can both can be considered as shift factors. The esterified sample, self-evidently, is located at a position 1;1. The data in Figure 12 can be described by a stretched exponential function covering the whole range from the esterified to the Rb^+-neutralized sample.

On the basis of the LRC-theory,[20] it is possible to calculate the characteristic lifetime of a telechelic association τ_t as

$$\tau_t \sim n^2 \tau_{term} \qquad (6)$$

where τ_{term} is the terminal relaxation time (in our case $\tau_{term} = 1/\omega_c$) and n the degree of functionalization since ($n = 2 \rightarrow 2$ ionic groups per molecule). The results are presented in Figure 13. For very low association levels, in particular for the acid precursor PBd(COOH)$_2$, the resulting characteristic lifetime is certainly also influenced by the reptation of the molecules, as the reptation time of the esterified sample is in the same ballpark as the characteristic lifetime. Hence, the 3.5 times longer terminal relaxation time of the acid precursor as compared to the esterified sample is a combination of reptation and association lifetime. On the contrary, for the alkali metal ions very long characteristic life times in the order of 10^{13} s (for $T_0 = T_g$) are found, which are only due to the ionic associations. (Figure 13).

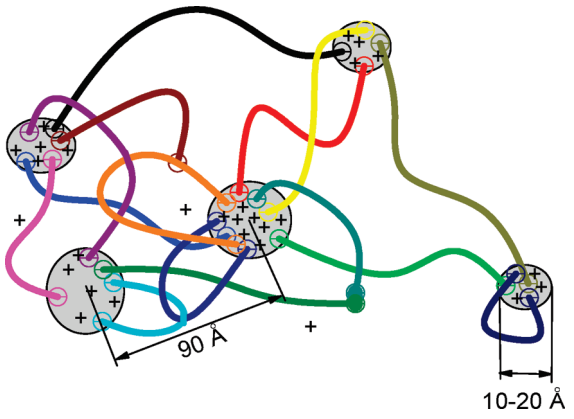

Figure 14. Tentative representation of the transient network structure of the neutralized samples.

The annealing effect mentioned earlier as an explanation for the discrepancy between the observed ion atomic number dependence and earlier published results, becomes quite obvious, when comparing the ratio between the crossover frequency of the Na^+-neutralized and acid precursor samples found here (7.8×10^6) vs the ratio found by Broze et al.[7] (167000). The ratios differ by a factor 47, using essentially the same base polymer.

This is a very important indicator that the time dependence can lead to dramatic effects and, thus, to apparent disagreement between published results in literature.

Conclusions

On the basis of the observations from SAXS and FT-IR as well as from the chemical composition knowledge, it is concluded that the neutralized samples consist of a biphasic structure. The main phase is the PBd main chain, but the end groups form clusters together with the counterions (Figure 14). Chain-ends can in principle form inter or intracluster associations. This is in agreement with the EHM model[4] developed for ionomers with randomly distributed ionic groups. These clusters are separated by about 85 Å—depending on the counterion, significantly less than the stretched chain length, which would be around 200 Å. This makes sense, as the stretched conformation is entropically very unfavorable.[19] The structure also roughly corresponds to the cluster structure previously reported for annealed zwitterionic telechelic polyisoprenes of the same number of entanglements.[19] FT-IR also shows the presence of small amounts of anhydrides in the sample, also schematically drawn in Figure 14.

The SAXS results show a clearer long period peak for the heavier ions, which correlates with the stronger ionic dipole observed by FT-IR. Although this correlation is indirect, it suggests that the stronger ionic dipoles observed for the heavier metals favor a higher degree of order in the cluster structure. The more perfect clusters show better cohesion, leading to longer terminal relaxation times, but also take much longer to equilibrate. The time needed to reach the equilibrium cluster structure is in the order of several months at room temperature and can only be characterized by comparing master curves obtained under equilibrium and out of equilibrium conditions. The strong ion dependence of the time to equilibrate the structure is the most probable reason for the apparent disagreement between literature and our data. The terminal relaxation time is not the reptation time of individual chains (which occur orders of magnitude faster except for the acid precursor), but the characteristic lifetime of a chain end attachment to an ionic cluster.

Besides the terminal relaxation, another relaxation process is the transition from the "upper" to the "lower" rubbery plateau, which becomes the stronger, the heavier the ion. This atomic mass dependence already is a good indicator of the physical background of the process. As stated before, heavy ions lead to a more perfect cluster structure and this means that the degree of "cross-linking" is higher, which increases the plateau modulus G_N^0. Consequently, this transition can be considered to be the consequence of a weakening of the cluster strength to a point that they can no longer be considered as cross-linkers. In other words, the transition between the two rubbery plateaus is the glass transition of the ionic aggregates and/or the motion arrested chains around them. This is the same process as already found for ionomers of a high ion content. In ionomers with a low ion content, however, no such glass transition has been observed. There are two possible explanations for this discrepancy. First, the secondary glass transitions were determined by DSC in literature, which is much less sensitive than melt or solid state rheology. Second, Figure 5 shows that this second glass transition does not appear clearly in an out-of-equilibrium sample. Most probably, the clear observation of two rubbery plateaus requires either a high ion content or a high degree of order (a well phase separated structure), which is very much time dependent.

Acknowledgment. The authors want to acknowledge financial support from the "Communauté Française de Belgique" and from the "Interuniversity Attraction Poles" program (IAP-PAI P6/27 "Functional Supramolecular Systems"). The help from Dr. Michaël Mainil and Mrs. Sabine Bebelman for the FT-IR experiments and from Mr. Pascal van Velthem for the SEC measurements is gratefully appreciated. J.-M.S. thanks the FRIA for financial support. C.-A.F. is a Research Associate of the FRS-FNRS. The authors would also like to thank Emerald Materials for supplying the diacid base polymer.

References and Notes

(1) Tant, M. R.; Mauritz, K. A.; Wilkes, G. L., *Ionomers - synthesis, structure, properties and applications*; Blackie Academics & Professional: London, 1997.
(2) Eisenberg, A.; Kim, J. S., *Introduction to Ionomers*; Wiley: New York, 1998.
(3) Galambos, A. F.; Stockton, W. B.; Koberstein, J. T.; Sen, A.; Weiss, R. A.; Russell, T. P. *Macromolecules* **1987**, *20*, 3091–3094.
(4) Eisenberg, A.; Hird, B.; Moore, R. B. *Macromolecules* **1990**, *23*, 4098–4107.
(5) Broze, G.; Jerome, R.; Teyssie, P. *Macromolecules* **1982**, *15*, 920–927.
(6) Davidson, N. S.; Fetters, L. J.; Funk, W. G.; Graessley, W. W.; Hadjichristidis, N. *Macromolecules* **1988**, *21*, 112–121.
(7) Broze, G.; Jerôme, R.; Teyssie, P. *Macromolecules* **1981**, *14*, 224–225.
(8) Broze, G.; Jerôme, R.; Teyssie, P.; Marco, C. *Macromolecules* **1983**, *16*, 1771–1775.
(9) Broze, G.; Jerôme, R.; Teyssie, P.; Marco, C. *Macromolecules* **1983**, *16*, 996–1000.
(10) Broze, G.; Jerôme, R.; Teyssie, P.; Marco, C. *Macromolecules* **1985**, *18*, 1376–1382.
(11) Fetters, L. J.; Graessley, W. W.; Hadjichristidis, N.; Kiss, A. D.; Pearson, D. S.; Younghouse, L. B. *Macromolecules* **1988**, *21*, 1644–1653.
(12) Register, R. A.; Prud'homme, R. E. Melt Rheology. In *Ionomers—synthesis, structure, properties and applications*; Tant, M. R., Mauritz, K. A., Wilkes, G. L., Eds. Blackie Academics & Professional: London, 1997.
(13) Antonietti, M.; Ehlich, D.; Foelsch, K. J.; Sillescu, H.; Schmidt, M.; Lindner, P. *Macromolecules* **1989**, *22*, 2802–2812.
(14) Antonietti, M.; Foelsch, K. J.; Sillescu, H.; Pakula, T. *Macromolecules* **1989**, *22*, 2812–2817.
(15) Grassl, B.; Billon, L.; Borisov, O.; Francois, J. *Polym. Int*. **2006**, *55*, 1169–1176.
(16) Hadjichristidis, N.; Pispas, S.; Pitsikalis, M. *Prog. Polym. Sci*. **1999**, *24*, 875–915.
(17) Karatzas, A.; Talelli, M.; Vasilakopoulos, T.; Pitsikalis, M.; Hadjichristidis, N. *Macromolecules* **2006**, *39*, 8456–8466.
(18) Karayianni, E.; Jerôme, R.; Cooper, S. L. *Macromolecules* **1997**, *30*, 7444–7455.
(19) Shen, Y.; Safinya, C. R.; Fetters, L.; Adam, M.; Witten, T.; Hadjichristidis, N. *Phys. Rev. A* **1991**, *43*, 1886–1891.
(20) Leibler, L.; Rubinstein, M.; Colby, R. H. *Macromolecules* **1991**, *24*, 4701–4707.
(21) Leibler, L.; Rubinstein, M.; Colby, R. H. *J. Phys. II* **1993**, *3*, 1581–1590.
(22) Leibler, L.; Rubinstein, M.; Colby, R. H. *Macromolecules* **1991**, *24*, 4701–4707.
(23) Tanaka, F.; Edwards, S. F. *Macromolecules* **1992**, *25*, 1516–1523.
(24) Rubinstein, M.; Semenov, A. N. *Macromolecules* **2001**, *34*, 1058–1068.
(25) Kujawa, P.; Audibert-Hayet, A.; Selb, J.; Candau, F. *Macromolecules* **2006**, *39*, 384–392.
(26) Clement, F.; Johner, A.; Joanny, J. F.; Semenov, A. N. *Macromolecules* **2000**, *33*, 6148–6158.
(27) van Ruymbeke, E.; Kapnistos, M.; Vlassopoulos, D.; Huang, T. Z.; Knauss, D. M. *Macromolecules* **2007**, *40*, 1713–1719.
(28) Pitsikalis, M.; Hadjichristidis, N. *Macromolecules* **1995**, *28*, 3904–3910.
(29) Connelly, R. W.; Mcconkey, R. C.; Noonan, J. M.; Pearson, G. H. *J. Polym. Sci., Part B: Polym. Phys*. **1982**, *20*, 259–268.
(30) Liu, C.; Bailly, C.; Yao, M.; Garritano, R. G.; Franck, A. J. Submitted for publication.
(31) Sternstein, S. S. *Adv. Chem. Ser*. **1983**, *203*, 123–147.
(32) Yarusso, D. J.; Cooper, S. L. *Macromolecules* **1983**, *16*, 1871–1880.
(33) Yarusso, D. J.; Cooper, S. L. *Polymer* **1985**, *26*, 371–378.
(34) Hosemann, R.; Bagchi, S. *Direct Analysis of Diffraction by Matter*; North Holland: Amsterdam, 1962.
(35) Matsuoka, H.; Tanaka, H.; Hashimoto, T.; Ise, N. *Phys. Rev. B* **1987**, *36*, 1754–1765.
(36) Matsuoka, H.; Tanaka, H.; Iizuka, N.; Hashimoto, T.; Ise, N. *Phys. Rev. B* **1990**, *41*, 3854–3856.
(37) Liu, C. Y.; Halasa, A. F.; Keunings, R.; Bailly, C. *Macromolecules* **2006**, *39*, 7415–7424.
(38) Juliani; Archer, L. A. *J. Rheol*. **2001**.
(39) Weiss, R. A.; Zhao, H. Y. *J. Rheol*. **2009**, *53*, 191–213.
(40) Folmer, B. J. B.; Sijbesma, R. P.; Versteegen, R. M.; van der Rijt, J. A. J.; Meijer, E. W. *Adv. Mater*. **2000**, *12*, 874–878.
(41) Hirschberg, J. H. K. K.; Beijer, F. H.; van Aert, H. A.; Magusim, P. C. M. M.; Sijbesma, R. P.; Meijer, E. W. *Macromolecules* **1999**, *32*, 2696–2705.
(42) Scherman, O. A.; Ligthart, G. B. W. L.; Ohkawa, H.; Sijbesma, R. P.; Meijer, E. W. *Proc. Natl. Acad. Sci. U.S.A*. **2006**, *103*, 11850–11855.
(43) Versteegen, R. M.; van Beek, D. J. M.; Sijbesma, R. P.; Vlassopoulos, D.; Fytas, G.; Meijer, E. W. *J. Am. Chem. Soc*. **2005**, *127*, 13862–13868.
(44) Stadler, F. J.; Keunings, R.; Bailly, C. In *Linear and Nonlinear Rheological Characterization of Difunctional Telechelic Polybutadienes*; 79th Annual Meeting of The Society of Rheology, Society of Rheology: Salt Lake City, UT, 2007.
(45) Vlassopoulos, D.; Pakula, T.; Fytas, G.; Pitsikalis, M.; Hadjichristidis, N. *J. Chem. Phys*. **1999**, *111*, 1760–1764.
(46) Vlassopoulos, D.; Pitsikalis, M.; Hadjichristidis, N. *Macromolecules* **2000**, *33*, 9740–9746.
(47) Fetters, L. J.; Lohse, D. J.; Colby, R. H., Chain Dimensions and Entanglement Spacings. In *Physical Properties of Polymers*, 2nd ed., Mark, J. E., Ed.; Springer: Heidelberg, Germany, 2007.
(48) Chassenieux, C.; Johannsson, R.; Durand, D.; Nicolai, T.; Vanhoorne, P.; Jerôme, R. *Colloids Surf. A: Physicochem. Eng. Asp*. **1996**, *112* (2−3), 155–162.
(49) Stadler, F. J.; Piel, C.; Kaminsky, W.; Münstedt, H. *Macromol. Symp*. **2006**, *236*, 209–218.
(50) Stadler, F. J.; Piel, C.; Klimke, K.; Kaschta, J.; Parkinson, M.; Wilhelm, M.; Kaminsky, W.; Münstedt, H. *Macromolecules* **2006**, *39*, 1474–1482.
(51) Weiss, R. A.; Fitzgerald, J. J.; Kim, D. *Macromolecules* **1991**, *24*, 1071–1076.
(52) Stadler, F. J.; Münstedt, H. *J. Rheol*. **2008**, *52*, 697–712.
(53) Stadler, F. J.; Piel, C.; Kaschta, J.; Rulhoff, S.; Kaminsky, W.; Münstedt, H. *Rheol. Acta* **2006**, *45*, 755–764.

(54) It is not possible to give a more precise value for G_N^0, as the thermorheological complexity around $\omega = 10^{-9}$ s^{-1} prevents the proper determination of the shift factors and the minimum in δ from whose position G_N^0 is determined.
(55) Trinkle, S.; Friedrich, C. *Rheol. Acta* **2001**, *40*, 322–328.
(56) Hartwig, G., *Polymer Properties at Room and Cryogenic Temperatures*; Plenum Press: New York, 1994.
(57) Liu, C. Y.; He, J. S.; Keunings, R.; Bailly, C. *Macromolecules* **2006**, *39*, 8867–8869.
(58) Stadler, F. J.; Bailly, C. *Rheol. Acta* **2009**, *48*, 33–49.
(59) Ngai, K. L.; Plazek, D. J. Temperature Dependences of the Viscoelastic Response of Polymer Systems. In *Physical Properties of Polymers Handbook*, 2nd ed.; Mark, J. E., Ed. Springer: Heidelberg, Germany, 2007.